

Circuit simulation using explicit methods

Mahesh B. Patil¹ and V.V.S. Pavan Kumar Hari²

¹Department of Electrical Engineering, Indian Institute of Technology Bombay

²Department of Energy Science and Engineering, Indian Institute of Technology Bombay

January 12, 2023

Abstract

Use of explicit methods for simulating electrical circuits, especially for power electronics applications, is described. Application of the forward Euler method to a half-wave rectifier is discussed, and the limitations of a fixed-step method are pointed out. Implementation of the Runge-Kutta-Fehlberg (RKF) method, which allows variable time steps, for the half-wave rectifier circuit is discussed, and its advantages pointed out. Formulation of circuit equations for the purpose of simulation using the RKF method is described for some more examples. Stability and accuracy issues related to power electronic circuits are brought out, and mechanisms to address them are presented. Future plans related to this work are described.

1 Introduction

Circuit simulation packages (e.g., NGSPICE [1], PSIM [2], PSCAD [3]) generally employ implicit methods, such as backward Euler and trapezoidal, for discretising the circuit equations involving time derivatives. Since these implicit methods are unconditionally stable, the simulator time steps are not constrained by stability issues. In other words, with these methods, the time step size is determined by accuracy considerations rather than stability constraints [4]. Therefore, even though they involve more work per time step, implicit methods are still the only practical option for circuits with very small time constants.

On the other hand, explicit methods, such as the Runge-Kutta-Fehlberg (RKF) [5] and Dormand-Prince (DP) [6] 4-5 pairs, involve less work per time step, and are ideally suited for non-stiff systems in which the time constants are not too small. Unfortunately, many circuits of practical interest do involve small time constants

arising from the small on-state resistance of a switch or a small capacitance associated with a semiconductor device. In such cases, a simulator using an explicit method is forced to take very small time steps although accuracy considerations would allow much larger time steps. Application of explicit methods to electronic circuits is therefore severely limited.

Power electronic circuits offer a unique opportunity to utilise the efficiency – due to smaller computational effort per time step – of explicit methods if the switches are treated as ideal. The simulator PLECS [7] exploits this idea to enable fast simulation of a variety of power electronic circuits. However, owing probably to the commercial nature of PLECS, hardly any details are available in the public domain about how the ideas broadly described in the PLECS 4.6 manual are actually implemented.

It is the purpose of this paper to discuss various issues related to the use of explicit methods for power electronic circuit simulation. We consider a few examples to illustrate the basic implementation scheme, the various challenges, and some ways to address them.

2 Half-wave rectifier

A half-wave rectifier circuit is shown in Fig. 1. In the

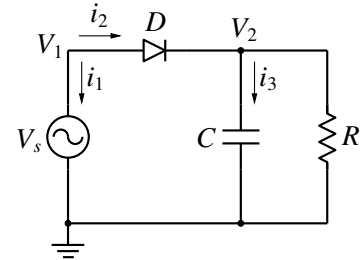


Figure 1: Half-wave rectifier circuit. The source voltage is given by $V_s = V_m \sin \omega t$.

following, we discuss how this circuit can be handled using an implicit method (backward Euler), an explicit method with a fixed time step (forward Euler), and an explicit method with a variable time step (RKF). The parameter values considered in all cases are: $V_m = 10$ V, $f = 50$ Hz, $C = 1$ mF, $R = 200$ Ω . The on-state voltage drop for the diode is taken to be $V_{on} = 0$ V.

2.1 Backward Euler (BE) method

The capacitor equation, $\frac{dV_C}{dt} = \frac{i_C}{C}$ is discretised using the BE method as,

$$\frac{V_{C,n+1} - V_{C,n}}{h} = \frac{i_{C,n+1}}{C}, \quad (1)$$

where X_n , X_{n+1} denote the numerically obtained value of X at $t = t_n$, $t = t_{n+1}$, respectively. In the context of the half-wave rectifier circuit, Eq. 1 gives,

$$i_{C,n+1} = \frac{C}{h} (V_{2,n+1} - V_{2,n}). \quad (2)$$

Using Eq. 2 and the Modified Nodal Analysis (MNA) approach [8] for assembling circuit equations, we get

$$i_{1,n+1} + G_D (V_{1,n+1} - V_{2,n+1}) = 0, \quad (3)$$

$$G_D (V_{2,n+1} - V_{1,n+1}) + \frac{C}{h} [V_{2,n+1} - V_{2,n}] + G V_{2,n+1} = 0, \quad (4)$$

$$V_{1,n+1} - V_m \sin \omega t_{n+1} = 0, \quad (5)$$

where $G = 1/R$. The diode has been modelled as $G_D = 1/R_D$, where $R_D = R_{on}$ if the diode is conducting, and $R_D = R_{off}$ if it is not. By making R_{on} and R_{off} sufficiently small and large, respectively, ideal diode behaviour can be realised.

Note that Eqs. 3-5 form a nonlinear set of equations (in $V_{1,n+1}$, $V_{2,n+1}$, $i_{1,n+1}$) since G_D is a nonlinear function of the diode voltage ($V_1 - V_2$). To solve this system of equations, circuit simulators generally employ the Newton-Raphson (N-R) iterative method in which the Jacobian equation must be solved for a few N-R iterations at each time point, thus making the procedure computationally expensive.

On the positive side, the backward Euler method is unconditionally stable and therefore does not impose an upper limit on the time step from the stability perspective. Furthermore, it allows complicated semiconductor device models to be incorporated in a straightforward manner.

2.2 Forward Euler (FE) method

The capacitor equation for the circuit of Fig. 1 can be discretised using the FE method as,

$$\frac{V_{2,n+1} - V_{2,n}}{h} = \frac{i_{3,n}}{C}. \quad (6)$$

Since $V_{2,n}$, $i_{3,n}$ are already known, $V_{2,n+1}$ can be found simply by evaluation, i.e.,

$$V_{2,n+1} = V_{2,n} + \frac{h}{C} i_{3,n}. \quad (7)$$

We can now obtain the rest of the variables at t_{n+1} by writing the circuit equations, treating $V_{2,n+1}$ as a *known* entity. The resulting equations can be written, for example, as

$$V_{1,n+1} - V_m \sin \omega t_{n+1} = 0, \quad (8)$$

$$i_{2,n+1} - G_D [V_{1,n+1} - V_{2,n+1}] = 0, \quad (9)$$

$$i_{2,n+1} - i_{3,n+1} - G V_{2,n+1} = 0, \quad (10)$$

a system of three equations in three variables: $V_{1,n+1}$, $i_{2,n+1}$, $i_{3,n+1}$. Note that G_D is still a nonlinear function of $(V_{1,n+1} - V_{2,n+1})$, making the situation similar to the backward Euler case.

In the interest of reducing the computation effort per time step, we now replace the original circuit with two circuits, one with the diode on, the other with the diode off, as shown in Fig. 2. Each of the two circuits is

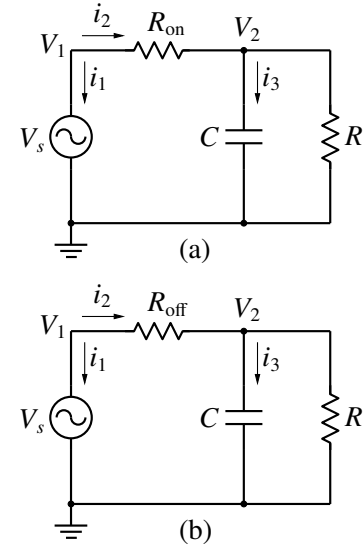


Figure 2: Circuit of Fig. 1 in two situations: (a) diode on, (b) diode off.

linear, with an associated set of equations (Eqs. 8-10), with $R_D = R_{on}$ in one case, and $R_D = R_{off}$ in the other.

Eqs. 8-10 can be written in the form $\mathbf{A} \mathbf{x} = \mathbf{b}$. For example, with the diode on, we have

$$\begin{bmatrix} 1 & 0 & 0 \\ -G_D^{\text{on}} & 1 & 0 \\ 0 & 1 & -1 \end{bmatrix} \begin{bmatrix} V_{1,n+1} \\ i_{2,n+1} \\ i_{3,n+1} \end{bmatrix} = \begin{bmatrix} V_m \sin \omega t_{n+1} \\ -G_D^{\text{on}} V_{2,n+1} \\ G V_{2,n+1} \end{bmatrix}, \quad (11)$$

where $G_D^{\text{on}} = 1/R_{\text{on}}$. Note that the time step h is not involved in the equations, and therefore the \mathbf{A} matrices are independent of time. This has a major implication, viz., \mathbf{A} and \mathbf{A}^{-1} for a specific switch configuration needs to be computed only once, offering a very significant speed-up with respect to an implicit method.

In some circuits, replacing a switch with R_{on} or R_{off} can create stability issues because R_{on} , a small resistance, can result in small RC -type time constants, and R_{off} , a large resistance, in small L/R -type time constants. In such cases, the simulator would be forced to take very small time steps. It is therefore preferable to make $R_{\text{on}} = 0$ and $R_{\text{off}} = \infty$, i.e., replace the switch with a short or open circuit.

In the half-wave rectifier circuit, using $R_{\text{on}} = 0$ creates a problem: The voltage source comes directly across the capacitor, and the \mathbf{A} matrix becomes singular. A slight modification of the circuit, viz., addition of a resistance R_1 in series with the capacitor, as shown in Fig. 3, circumvents this problem. The resistance R_1 should be small (taken as $10 \text{ m}\Omega$ in this paper) so that it does not change the circuit operation.

There are different ways in which the set of equations for the on and off circuits of Fig. 3 can be written. In the following, we opt for a systematic procedure which can be easily extended to other circuits. We write the KCL equations at all nodes except the reference node, followed by the element equations. Note that

$$V_{C,n+1} = V_{C,n} + \frac{1}{C} i_{3,n} \quad (12)$$

is treated as a known value. The set of equations is then given by

$$i_{1,n+1} + i_{2,n+1} = 0, \quad (13)$$

$$-i_{2,n+1} + i_{3,n+1} + i_{5,n+1} = 0, \quad (14)$$

$$-i_{3,n+1} + i_{4,n+1} = 0, \quad (15)$$

$$V_{1,n+1} = V_m \sin \omega t_{n+1}, \quad (16)$$

$$V_{2,n+1} - V_{3,n+1} = V_{C,n+1}, \quad (17)$$

$$i_{4,n+1} - G_1 V_{3,n+1} = 0, \quad (18)$$

$$i_{5,n+1} - G V_{2,n+1} = 0, \quad (19)$$

$$\begin{aligned} V_{1,n+1} - V_{2,n+1} &= 0 & \text{if } D \text{ is on,} \\ i_{2,n+1} &= 0 & \text{if } D \text{ is off.} \end{aligned} \quad (20)$$

Eqs. 13-20 can be described in a matrix form, $\mathbf{A} \mathbf{x} = \mathbf{b}$, where the solution vector \mathbf{x} consists of $V_{1,n+1}$, $V_{2,n+1}$, $V_{3,n+1}$, $i_{1,n+1}$, $i_{2,n+1}$, $i_{3,n+1}$, $i_{4,n+1}$, $i_{5,n+1}$, and \mathbf{b} includes $V_{C,n+1}$ and $V_{s,n+1}$, both being known values. Since the circuit has one switch, we have two possible \mathbf{A} matrices, $\mathbf{A}^{(\text{on})}$ and $\mathbf{A}^{(\text{off})}$, corresponding to the diode in the on and off state, respectively. In general, the number of \mathbf{A} matrices would be 2^N , where N is the number of switches in the circuit. After solving $\mathbf{A} \mathbf{x} = \mathbf{b}$, we need to make sure that the diode state is consistent with the \mathbf{A} matrix which was used in the computation. For example, in the half-wave rectifier case, if $\mathbf{A}^{(\text{off})}$ was used, then $i_{2,n+1}$ must turn out to be positive. If it is not, we need to reject the solution, use $\mathbf{A}^{(\text{on})}$ instead, and solve $\mathbf{A} \mathbf{x} = \mathbf{b}$ again. If $\mathbf{A}^{(\text{on})}$ has already been computed (and stored) earlier, solving $\mathbf{A} \mathbf{x} = \mathbf{b}$ takes a small computational effort.

Note that it is not necessary to pre-compute the \mathbf{A} and \mathbf{A}^{-1} matrices for all 2^N switch configurations. In many power electronic circuits, only a small fraction of the switch configurations get actually visited, and pre-computing (and storing) all possible \mathbf{A} and \mathbf{A}^{-1} matrices would be wasteful in terms of time and memory. Instead, the matrices should be computed and stored dynamically, i.e., whenever a specific switch configuration is encountered. The overall procedure can be summarised as shown in Algorithm 1. We will refer to this scheme of using an explicit method for electrical circuits as the ELEX (ELEctrical EXplicit) scheme. For reasons explained in the following, the FE method is not a good candidate for the ELEX scheme. Instead, a variable time-step method (for example, RKF or DP) would be preferred.

Algorithm 1 ELEX scheme

- 1: Initialise switch state vector (\mathbf{S}).
 - 2: $t \leftarrow 0$
 - 3: **while** $t < t_{\text{end}}$ **do**
 - 4: Update source outputs.
 - 5: Update state variables.
 - 6: Compute \mathbf{b}
 - 7: **if** $\nexists \mathbf{A}(\mathbf{S})$ **then**
 - 8: Compute $\mathbf{A}(\mathbf{S})$ and $\mathbf{A}^{-1}(\mathbf{S})$.
 - 9: **end if**
 - 10: Solve $\mathbf{A} \mathbf{x} = \mathbf{b}$.
 - 11: Compute \mathbf{S}_{new} (new switch states)
 - 12: **if** $\mathbf{S} \neq \mathbf{S}_{\text{new}}$ **then**
 - 13: Pick new \mathbf{S} .
 - 14: Go to 7
 - 15: **end if**
 - 16: **end while**
-

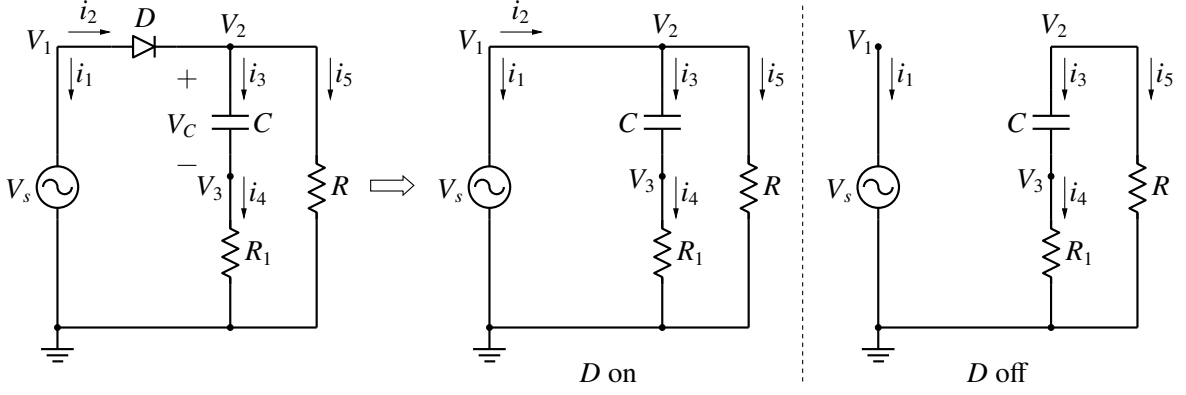


Figure 3: Addition of R_1 in series with C in the half-wave rectifier circuit of Fig. 1, and the equivalent circuits when the diode is on or off.

We now comment on stability issues related to the FE method when applied to the circuit of Fig. 3. The charging and discharging time constants, τ_1 and τ_2 , are given by

$$\tau_1 = (R_1 \parallel R) C \simeq R_1 C = 10 \mu\text{sec}, \quad (21)$$

$$\tau_2 = (R_1 + R) C \simeq R C = 0.2 \text{ sec}. \quad (22)$$

The FE method becomes unstable when the time step h is larger than 2τ . Clearly, we need to use h smaller than $2\tau_1$ or $20 \mu\text{sec}$ in the charging phase. Since the FE method is a fixed time step method, we end up using this small time step ($20 \mu\text{sec}$) *throughout* the simulation, requiring at least $T/\tau_1 = 20 \text{ msec}/20 \mu\text{sec}$ or 10^3 time points in one period. From the accuracy point, such a large number of time steps is not required, and the FE method is therefore too slow for many applications.

The stability problem is illustrated in Figs. 4 and 5. When $h < 20 \mu\text{sec}$ is used (Fig. 4), the simulation results are as expected. For $h = 20 \mu\text{sec}$ (Figs. 5 and 6), oscillations can be seen in the diode current, indicating unstable behaviour of the FE method.

2.3 Runge-Kutta-Fehlberg (RKF) method

The RKF method is an adaptive (variable) time step method in which a Runge-Kutta method of order four is used together with a Runge-Kutta method of order five to obtain an estimate of the local truncation error (LTE) in a given time step. If the LTE is smaller than a user-specified tolerance, the next time step is allowed to be larger than the current time step. On the other hand, if the LTE is larger than the tolerance, then the current time step is rejected, and a smaller time step is tried. The RKF method requires more work at each time step (six function evaluations) as compared to the FE method (one

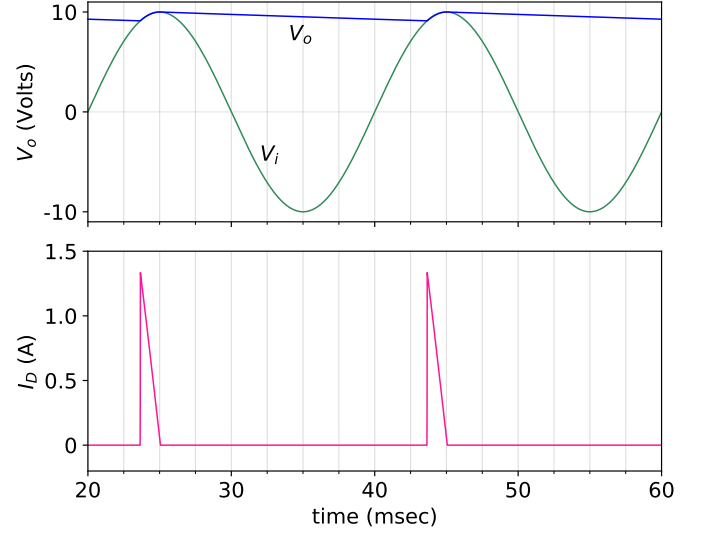


Figure 4: Input and output voltages, and diode current obtained with the FE method for the half-wave rectifier circuit of Fig. 3 with time step $h = 10 \mu\text{sec}$.

function evaluation). However, its auto time step feature allows a dramatic reduction in the total number of time points required for the simulation while simultaneously satisfying the LTE constraint, and it is therefore much more efficient than the FE method.

The RKF method for a single ordinary differential equation (ODE) $\frac{dx}{dt} = f(t, x)$ can be described as follows. First, compute k_1, k_2, \dots, k_6 as,

$$k_1 = h f(t_n, x_n), \quad (23)$$

$$k_2 = h f(t_n + \alpha_2 h, x_n + \beta_{2,1} k_1), \quad (24)$$

$$k_3 = h f(t_n + \alpha_3 h, x_n + \sum_{j=1}^2 \beta_{3,j} k_j), \quad (25)$$

$$k_4 = h f(t_n + \alpha_4 h, x_n + \sum_{j=1}^3 \beta_{4,j} k_j), \quad (26)$$

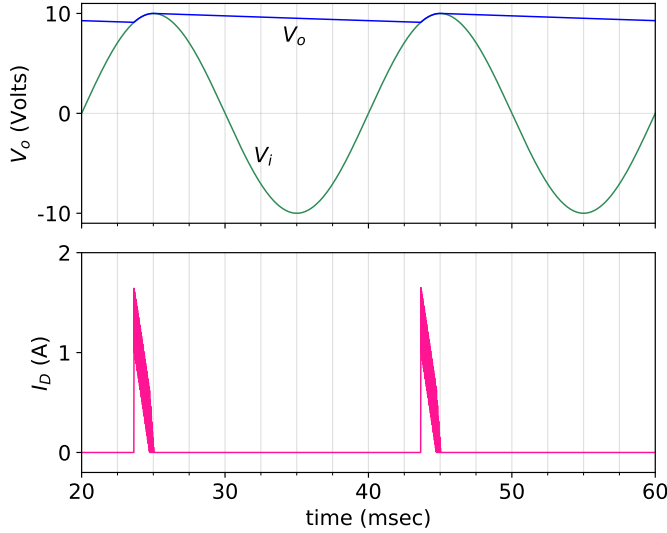


Figure 5: Input and output voltages, and diode current obtained with the FE method for the half-wave rectifier circuit of Fig. 3 with time step $h = 20 \mu\text{sec}$.

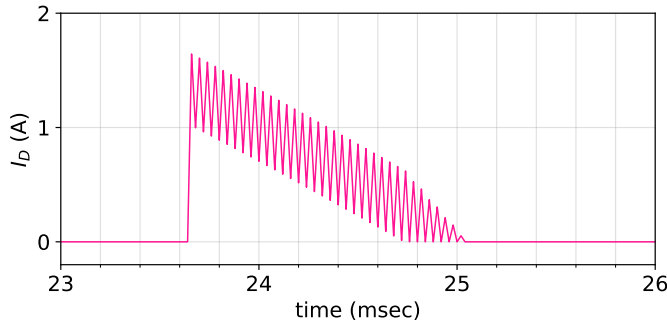


Figure 6: Diode current obtained with the FE method for the half-wave rectifier circuit of Fig. 3 with time step $h = 20 \mu\text{sec}$.

$$k_5 = h f(t_n + \alpha_5 h, x_n + \sum_{j=1}^4 \beta_{5,j} k_j), \quad (27)$$

$$k_6 = h f(t_n + \alpha_6 h, x_n + \sum_{j=1}^5 \beta_{6,j} k_j), \quad (28)$$

where $\alpha_i \leq 1$. The fourth- and fifth-order estimates for x_{n+1} are then given by

$$x_{n+1} \text{ (4th order)} = x_n + \sum_{j=1}^5 \gamma_j^{(4)} k_j, \quad (29)$$

$$x_{n+1} \text{ (5th order)} = x_n + \sum_{j=1}^6 \gamma_j^{(5)} k_j. \quad (30)$$

The constants α, β, γ in the above equations can be found in [5]. The difference between the fourth- and fifth-order x_{n+1} values gives an estimate of the LTE. If the LTE is smaller than a tolerance, then the fifth order x_{n+1} value is

accepted as the numerical solution of the ODE at t_{n+1} ; if not, the current time step is rejected, and a revised value of h is computed, using the LTE estimate [5].

For the half-wave rectifier of Fig. 3, the ODE comes from the capacitor and is given by

$$\frac{dV_c}{dt} = \frac{1}{C} i_3 \quad (31)$$

(see Fig. 3). The first step in applying the RKF method to this problem is to compute k_1 (see Eq. 23) as

$$k_1 = h \frac{1}{C} i_{3,n}, \quad (32)$$

where $i_{3,n}$ is the numerical solution for i_3 at t_n and is already known. For the next RKF step (Eq. 24), we compute an intermediate value of i_3 (denoted by $i_3^{(2)}$) using the following steps.

(i) Update $V_C^{(2)}$ as

$$V_C^{(2)} = V_{C,n} + \beta_{2,1} k_1. \quad (33)$$

(ii) Update $V_s^{(2)}$ as

$$V_s^{(2)} = V_m \sin \omega (t_n + \alpha_2 h). \quad (34)$$

(iii) Solve the following set of equations, making sure that the \mathbf{A} matrix (corresponding to diode on or off) used for solving the equations is consistent with the solution.

$$i_1^{(2)} + i_2^{(2)} = 0, \quad (35)$$

$$-i_2^{(2)} + i_3^{(2)} + i_5^{(2)} = 0, \quad (36)$$

$$-i_3^{(2)} + i_4^{(2)} = 0, \quad (37)$$

$$V_1^{(2)} = V_s^{(2)} \quad (38)$$

$$V_2^{(2)} - V_3^{(2)} = V_C^{(2)}, \quad (39)$$

$$i_4^{(2)} - G_1 V_3^{(2)} = 0, \quad (40)$$

$$i_5^{(2)} - G V_2^{(2)} = 0, \quad (41)$$

$$\begin{aligned} V_1^{(2)} - V_2^{(2)} &= 0 & \text{if } D \text{ is on,} \\ i_2^{(2)} &= 0 & \text{if } D \text{ is off.} \end{aligned} \quad (42)$$

We are now in a position to compute k_2 and $V_C^{(3)}$ as

$$k_2 = h \frac{1}{C} i_3^{(2)}, \quad (43)$$

$$V_C^{(3)} = V_C^{(2)} + \beta_{3,1} k_1 + \beta_{3,2} k_2. \quad (44)$$

We then compute $V_s^{(3)}$ as $V_m \sin \omega(t_n + \alpha_3 h)$, solve the circuit equations to obtain $i_3^{(3)}$, and compute k_3 . Proceeding in this manner, we compute k_1, k_2, \dots, k_6 , and finally the fourth- and fifth-order estimates for $V_{C,n+1}$ (Eqs. 29 and 30). If there are several capacitors and inductors in the circuit, we would evaluate Eq. 33 for each of the state variables (inductor currents and capacitor voltages), update source value(s), and then solve the electrical equations.

Fig. 7 shows the results obtained with the RKF method. The time points used by the RKF method are shown by crosses in the $V_i(t)$ plot. It can be seen that, in the charging phase (where the time constant is small), small time steps are taken by the RKF method. In the discharging phase, the time constant is large, and much larger time steps – limited in this case by a user-specified maximum time step of 0.5 msec – are taken by the RKF method, thus leading to a much smaller number of total time points, as compared to the FE method.

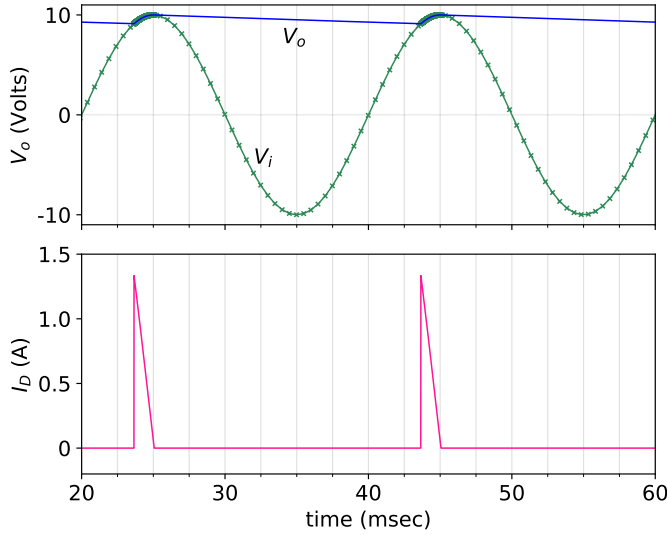


Figure 7: Input and output voltages, and diode current obtained with the RKF method for the half-wave rectifier circuit of Fig. 3. The simulation time points are shown by crosses in the V_i plot.

The half-wave rectifier example brings out the fundamental limitation of using explicit methods for electrical circuits, viz., the necessity of using small time steps because of stability constraints. However, in several power electronic circuits of interest, the ELEX scheme essentially bypasses the stability issue by avoiding small time constants altogether, and in that case, the time step is limited by accuracy, rather than stability.

3 Switches in series

Consider the controlled switch, e.g., an idealised MOS transistor, shown in Fig. 8 (a). In the ELEX scheme, we

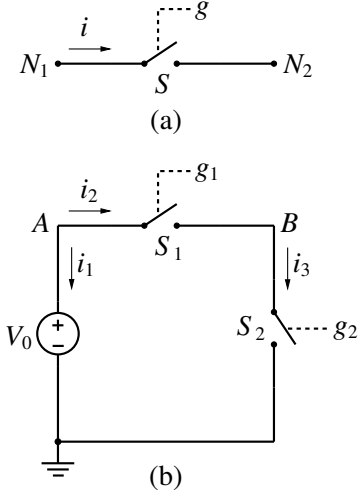


Figure 8: (a) Schematic diagram of a controlled switch, (b) A circuit with two controlled switches in series.

can write the switch equation as

$$\begin{aligned} V_{N1} - V_{N2} &= 0 & \text{if } D \text{ is on,} \\ i &= 0 & \text{if } D \text{ is off.} \end{aligned} \quad (45)$$

In most situations, the above approach would work fine. However, this simple model can fail for some specific situations. As an example, consider the circuit shown in Fig. 8 (b) in which V_0 is a dc (known) voltage. If $g_1 = 1$ and $g_2 = 0$, we expect $V_B = V_0$. If $g_1 = 0$ and $g_2 = 1$, we expect $V_B = 0$ (see Fig. 9). When both g_1 and g_2 are zero, we would expect the applied voltage V_0 to split equally between the two switches, and V_B should therefore be 5 V, as shown in Fig. 9. Let us now apply the ELEX scheme to this circuit.

Once again, we write the equations in a systematic manner, writing the KCL equations first, followed by the element equations, and get

$$i_1 + i_2 = 0, \quad (46)$$

$$i_2 - i_3 = 0, \quad (47)$$

$$V_A = V_0, \quad (48)$$

$$\begin{aligned} V_A - V_B &= 0 & \text{if } g_1 = 1, \\ i_2 &= 0 & \text{if } g_1 = 0, \end{aligned} \quad (49)$$

$$\begin{aligned} V_B &= 0 & \text{if } g_2 = 1, \\ i_3 &= 0 & \text{if } g_2 = 0, \end{aligned} \quad (50)$$

where we have applied Eq. 45 to each of the two switches.

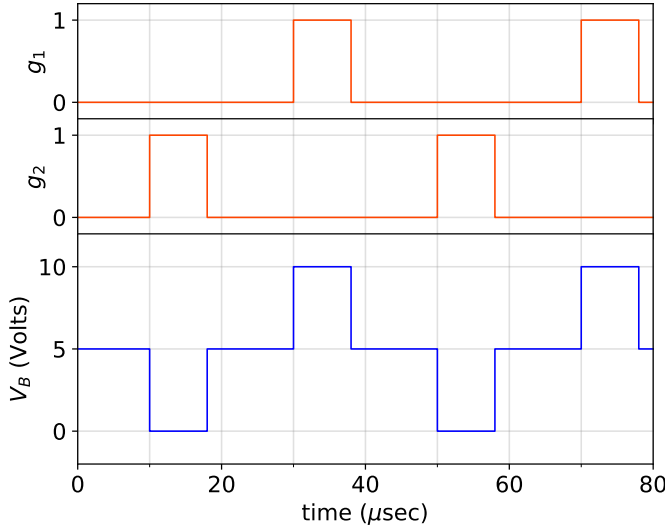


Figure 9: Sample waveforms expected for the circuit of Fig. 8 (b) with $V_0 = 10$ V.

If one of g_1 and g_2 is high, Eqs. 46-50 give us the expected result. For the case $g_1 = g_2 = 0$, no solution is possible because node B becomes isolated. In other words, if the equations are written in the form $\mathbf{A} \mathbf{x} = \mathbf{b}$, then \mathbf{A} turns out to be singular. Although this situation is rare in power electronic circuits, a general-purpose simulation program must be able to handle it suitably.

When both S_1 and S_2 are off, we expect V_0 to divide equally between them, which suggests that the switch should be modelled as a large resistance R_{off} in the off state. However, in the ELEX scheme, we would like to avoid such a representation because of its potential to create small L/R -type time constants. What we need is a procedure that allows voltage division between the switches, but without replacing the switch with R_{off} . One way to achieve these conflicting goals is as follows.

When the gate voltage is high, we continue to model the switch with the ideal switch equation

$$V_{N1} - V_{N2} = 0. \quad (51)$$

When the gate voltage is low, we use the model shown in Fig. 10, where $G' = 1/R_{\text{off}}$ is a small conductance.

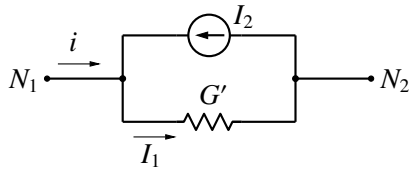


Figure 10: Equivalent circuit of a controlled switch in the off state for implementation in the ELEX scheme.

The current I_2 is given by,

$$I_2 = \frac{k-1}{k_{\text{max}}-1} G' (V_{N1} - V_{N2}), \quad (52)$$

where k takes values, $1, 2, \dots, k_{\text{max}}$. The switch current i in the off state is then given by

$$i - G' (V_{N1} - V_{N2}) = -\frac{k-1}{k_{\text{max}}-1} G' (V_{N1} - V_{N2}). \quad (53)$$

With $k = 1$, Eq. 53 amounts to removing the current source I_2 in Fig. 10, keeping only G' . When the circuit equations are solved for this condition, voltages get suitably assigned. For the example of Fig. 8 (b), we would get $V_B = V_0/2$. When $k = k_{\text{max}}$, Eq. 53 reduces to $i = 0$, the ideal switch equation in the off state, since I_1 and I_2 become equal. Thus, by increasing k from 1 to k_{max} , we achieve our objective of establishing appropriate node voltages without replacing the switch with R_{off} . For the circuit of Fig. 8 (b), $k_{\text{max}} = 2$ is adequate. It remains to be seen if a larger value of k_{max} is necessary for some other circuits.

Eq. 53, for a given value of k , is solved in an iterative manner, treating V_{N1} , V_{N2} on the right-hand side (RHS) as known values coming from the previously computed solution. The RHS becomes part of \mathbf{b} in $\mathbf{A} \mathbf{x} = \mathbf{b}$, the complete set of circuit equations. Solving $\mathbf{A} \mathbf{x} = \mathbf{b}$, we obtain revised values of V_{N1} , V_{N2} , and use those to compute the RHS of Eq. 53 again, and so on until convergence. For the circuit of Fig. 8 (b), two iterations suffice.

Clearly, the above procedure comes with an additional computational cost and should therefore be used only if the ideal switch model (Eq. 45) is creating a singular matrix situation. In most power electronic circuits, the ideal switch model seems to work well.

4 Boost converter

Consider the boost converter circuit shown in Fig. 11. For the parameter values given in the figure, the inductor current (in the steady state) is discontinuous, as shown in Fig. 12. The purpose of this section is to describe the challenges presented by the discontinuous nature of the inductor current and to present a way to address the same.

The ELEX-RKF procedure to obtain the solution at t_{n+1} – assuming as always the solution at t_n to be already available – starts with

$$k_1^{(C)} = h \frac{1}{C} i_{5,n}, \quad (54)$$

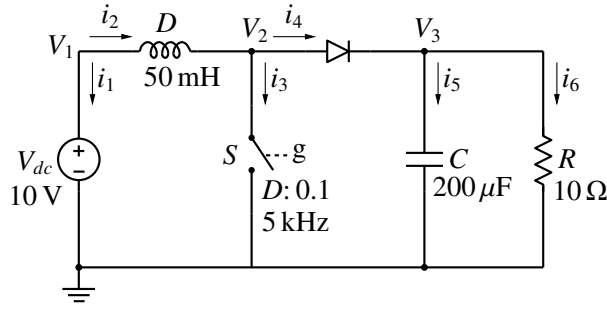


Figure 11: Boost converter circuit.

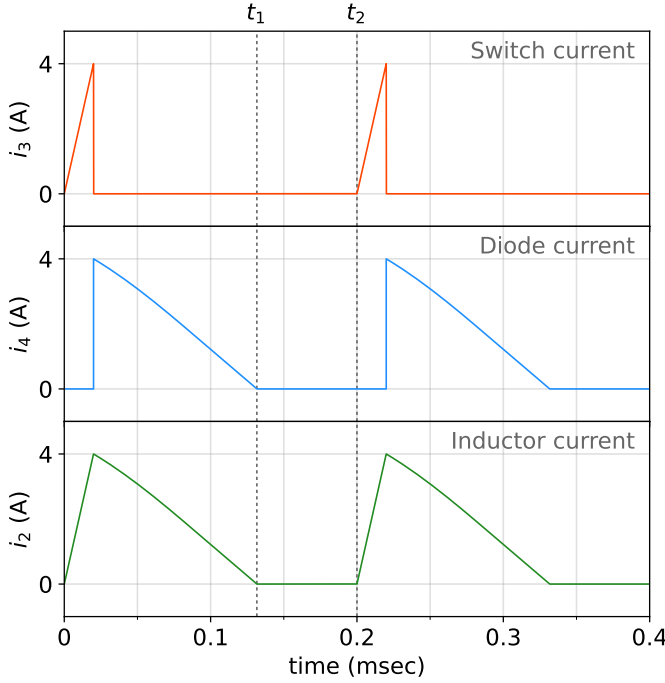


Figure 12: Steady-state waveforms for the boost converter circuit of Fig. 11.

$$k_1^{(L)} = h \frac{1}{L} V_{L,n}, \quad (55)$$

for the capacitor and inductor, respectively. The inductor voltage V_L for this circuit is $V_L = V_1 - V_2$.

Next, we obtain $V_C^{(2)}$ and $i_L^{(2)}$, the phase-2 updates for V_C and i_L , as

$$V_C^{(2)} = V_{C,n} + \beta_{2,1} k_1^{(C)}, \quad (56)$$

$$i_L^{(2)} = i_{L,n} + \beta_{2,1} k_1^{(L)}, \quad (57)$$

update the gate voltage value for the MOS switch, and then solve the set of circuit equations given by

$$i_1^{(2)} + i_2^{(2)} = 0, \quad (58)$$

$$i_2^{(2)} - i_3^{(2)} - i_4^{(2)} = 0, \quad (59)$$

$$i_4^{(2)} - i_5^{(2)} - i_6^{(2)} = 0, \quad (60)$$

$$V_1^{(2)} = V_{dc}, \quad (61)$$

$$i_2^{(2)} = i_L^{(2)}, \quad (62)$$

$$V_3^{(2)} = V_C^{(2)}, \quad (63)$$

$$i_6^{(2)} - G V_3^{(2)} = 0, \quad (64)$$

$$i_4^{(2)} - i_d^{(2)} = 0, \quad (65)$$

$$i_3^{(2)} - i_{sw}^{(2)} = 0, \quad (66)$$

$$\begin{aligned} V_2^{(2)} - V_3^{(2)} &= V_{on} \quad \text{if } D \text{ is on,} \\ i_d^{(2)} &= 0 \quad \text{if } D \text{ is off,} \end{aligned} \quad (67)$$

$$\begin{aligned} V_2^{(2)} &= 0 \quad \text{if } S \text{ is on,} \\ i_{sw}^{(2)} &= 0 \quad \text{if } S \text{ is off.} \end{aligned} \quad (68)$$

Having obtained the solution at stage 2 of the RKF process, we then proceed to compute $k_2^{(C)}$, $k_2^{(L)}$, solve the circuit equations to obtain the solution at stage 3, and so on. In a way, this is a straightforward extension of the ELEX-RKF scheme we have seen in Sec. 2.3. However, one major change is required.

In the interval from t_1 to t_2 in Fig. 12, both S and D are off, i.e., $i_3 = i_4 = 0$. With this condition, the $\mathbf{A} \mathbf{x} = \mathbf{b}$ problem described by Eqs. 58-68 has no solution because \mathbf{A} becomes singular. Intuitively, we would expect that to happen since we are trying to assign a value to the inductor current when there is no path for that current. Even a boost converter which has continuous conduction in the steady state can go through the above situation (where both D and S are simultaneously off) in the transient phase, i.e., before steady state is attained by the circuit.

The singular matrix issue can be addressed by connecting a resistance R_p in parallel with L as shown in Fig. 13. The R_p value should be chosen to be sufficiently

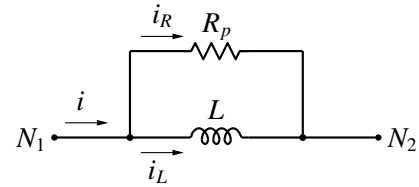


Figure 13: Addition of a resistance in parallel with an inductor to address the singular matrix issue (see text).

large (say, 1 MΩ) such that it draws a negligibly small current, thus leaving the circuit solution essentially undisturbed. With R_p in place, the inductor current equation (Eq. 62) gets replaced by

$$i_2^{(2)} - (V_1^{(2)} - V_2^{(2)})/R_p = i_L^{(2)}, \quad (69)$$

and the circuit matrix \mathbf{A} remains non-singular even if i_3 and i_4 in Fig. 11 become zero.

The turn-off process of the diode at time t_1 (see Fig. 12) needs to be carefully handled for the following reason. The inductor current in the ELEX-RKF scheme gets updated in several stages of the RKF process, the first step being

$$i_L^{(2)} = i_{L,n} + \beta_{2,1} \frac{h}{L} V_{L,n}, \quad (70)$$

where $i_{L,n}$ and $V_{L,n}$ come from the solution obtained at $t = t_n$. It is crucial to catch the diode turn-off point as closely as possible, i.e., the diode current should be sufficiently small before we move on to the off condition of the diode. This is achieved in the ELEX scheme using binary search – as in the PLECS [7] program – where we keep narrowing the bracket around the exact turn-off point, until it becomes acceptably small, say, $\Delta t = 10^{-12}$ sec. When that is achieved, we have two simulation time points, one before and one after the turn-off event, the interval between them being Δt . Let us denote these two points by t'_{on} and t'_{off} . At t'_{on} , the diode is still on, but i_d (i_4 in Fig. 11) is small, say, 10^{-12} A or smaller. At t'_{off} , the diode has turned off, i_d is exactly zero, and KCL implies that i_2 (in Fig. 11) is also zero, since the MOS switch is already off. The currents i_L and i_R in Fig. 13 at $t = t'_{\text{off}}$ cancel each other exactly. These currents are individually small but not zero. Considering this situation, in order to ensure that i_L goes to zero quickly, we can use

$$i_L^{(2)} = i_{2,n} + \beta_{2,1} \frac{h}{L} V_{L,n}, \quad (71)$$

rather than Eq. 70. Note that $i_{L,n}$ has been replaced with $i_{2,n}$ on the right-hand side in Eq. 71.

With the above modification, the ELEX-RKF scheme was able to handle the boost converter circuit of Fig. 11 accurately. It was observed that, if the diode current at t'_{on} is not small enough, the inductor current does not reduce to zero. As we proceed to the off state of the diode, we have a situation in which both the diode and MOS switch are off, and $i_L = -i_R$ (Fig. 13). In other words, current circulates in the L - R_p loop. This is a disastrous situation because the small time constant L/R_p of the L - R_p loop forces the RKF process to take very small time steps, and the simulation becomes impractically slow.

In a general scenario, the L - R_p combination is useful in another sense. If a substantial inductor current is forced to become zero abruptly, the current would then go through R_p , causing an unrealistically large voltage drop across the inductor. This voltage drop can be

monitored by the simulator to issue a suitable warning or error message.

5 Closed-loop circuits

In a closed-loop power electronic circuit, additional variables related to the control block are involved. Typically, the electrical circuit produces one or more feedback quantities (currents or voltages), which serve as inputs to the control block, as shown in Fig. 14. The

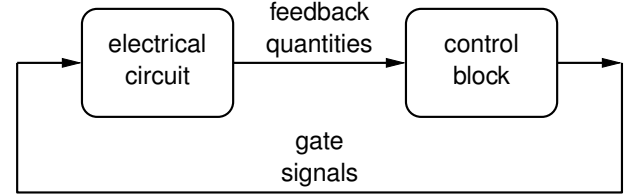


Figure 14: Typical structure of a closed-loop power electronic circuit.

control block in turn generates the gate signals required by the electrical circuit. In general, the control block is easier to handle than the electrical block because it involves only a “flow graph” and not a network where KCL and KVL equations need to be satisfied. When an explicit method is used to handle the control block, as we would be doing in the ELEX-RKF scheme, several “passes” are made to treat the elements of the control block, as dictated by the flow graph (see [9], [10]). In each pass, only those elements whose input values have been updated are processed. In the following, we will consider two examples to illustrate how the ELEX-RKF scheme can be applied to closed-loop circuits.

5.1 Current-controlled two-level voltage source converter

The circuit diagram for a current-controlled two-level voltage source converter is shown in Fig. 15, along with the control block. We have already seen how voltage sources, MOS switches, resistors, inductors, are treated in the ELEX-RKF scheme. Let us see how the two new electrical elements in this circuit, viz., ammeter and voltmeter, can be handled. The ammeter is like a dc voltage source with $V_{dc} = 0$ V, satisfying the equations,

$$V_{P2} - V_{P3} = 0. \quad (72)$$

$$i_9 - i_{fb} = 0, \quad (73)$$

The voltmeter is like a dc current source with $I_{dc} = 0$ A, satisfying the equations,

$$i_{11} = 0, \quad (74)$$

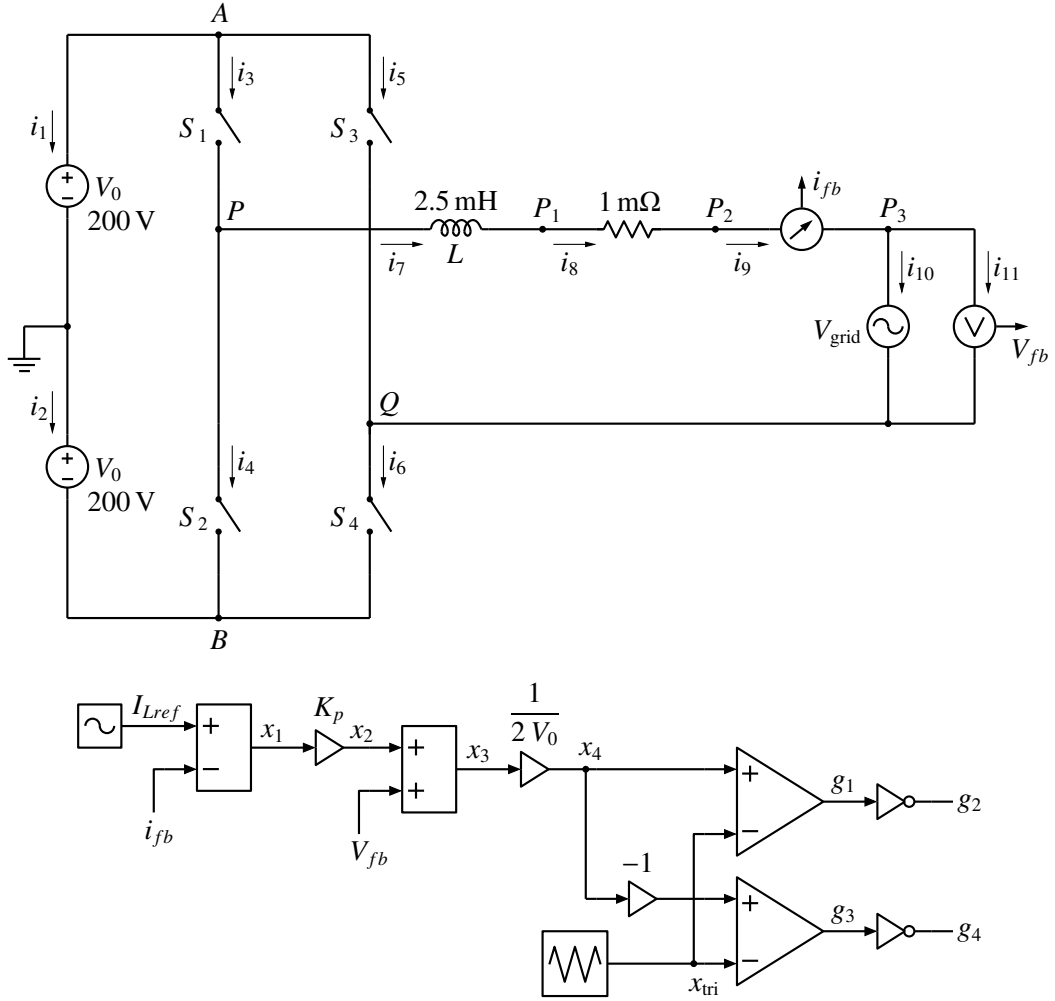


Figure 15: Schematic diagram of current-controlled two-level voltage source converter. The reference current is given by $I_{Lref} = I_m \sin(\omega t + \phi)$, where $I_m = 2.5\sqrt{2}$ A, $f = 50$ Hz, $\phi = -\pi/6$. The triangular waveform is symmetric, with minimum and maximum values of -1 and 1 , respectively, and $f_{tri} = 20$ kHz. K_p is given by $K_p = \omega_{tri}L/10$.

$$V_{P3} - V_Q - V_{fb} = 0. \quad (75)$$

The element equations, together with the KCL equations, constitute the set of electrical equations which, as we have seen in Sec. 4, can be written in the form $\mathbf{A} \mathbf{x} = \mathbf{b}$. Note that the feedback variables, i_{fb} and V_{fb} , are also included in \mathbf{x} .

At each stage of the RKF process, we solve the electrical equations and obtain i_{fb} , V_{fb} . This is followed by updating the “control” variables I_{Lref} , x_{tri} , x_1 , x_2 , x_3 , x_4 , and finally the gate signals g_1 to g_4 . In this example, the control block does not involve any state variables.

The control variables are updated as follows. First, we treat the source elements by assigning suitable values to I_{Lref} and x_{tri} . The rest of the control variables are then updated as

$$x_1 = I_{Lref} - i_{fb}, \quad (76)$$

$$x_2 = K_p x_1, \quad (77)$$

$$x_3 = x_2 - V_{fb}, \quad (78)$$

$$x_4 = \frac{1}{2V_0} x_3. \quad (79)$$

The gate signals g_1 to g_4 are then obtained by comparing x_4 or $-x_4$ with x_{tri} .

In the interest of resolving the gate signal waveforms accurately, the simulator time steps are limited by placing additional time points before and after the expected cross-over points of the comparators, as described in [11]. Simulation results obtained for $i_{fb}(t)$ are shown in Fig. 16, along with the reference current $I_{Lref}(t)$. The two currents are shown on an expanded scale in Fig. 17.

Simulation results obtained for $i_{fb}(t)$, when the comparator cross-over time points are not treated accurately (with all other simulation parameters the same), are shown in Fig. 18. By comparing Figs. 16 and 18, we can clearly see that simulation accuracy is

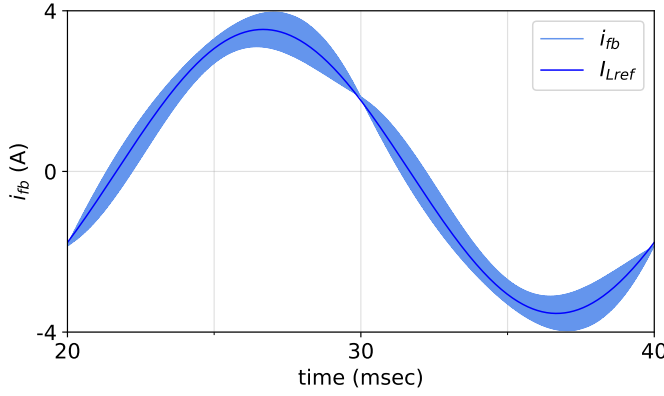


Figure 16: ELEX-RKF results for the current-controlled two-level voltage source converter of Fig. 15.

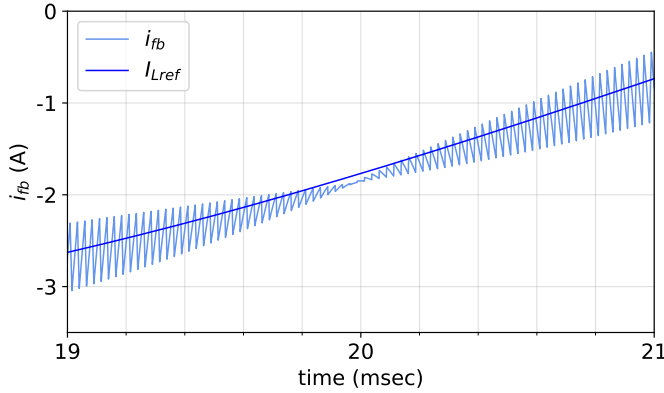


Figure 17: ELEX-RKF results for the current-controlled two-level voltage source converter of Fig. 15 on an expanded scale.

significantly affected by correct treatment of comparator cross-over.

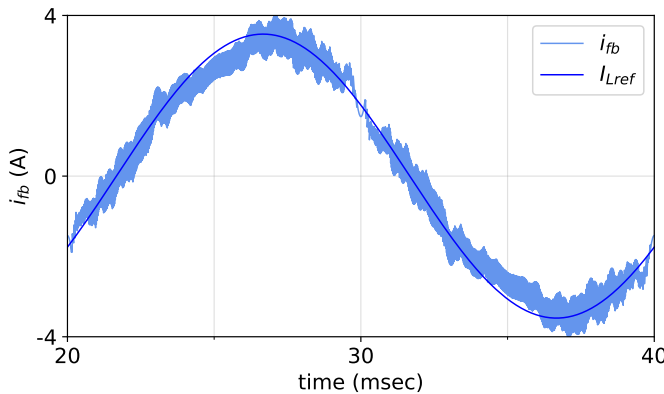


Figure 18: ELEX-RKF results for the current-controlled two-level voltage source converter of Fig. 15, when comparator cross-over points are not treated accurately.

5.2 Voltage-controlled buck DC-DC converter

Fig. 19 shows a voltage-controlled buck DC-DC converter, with the voltage reference V_{ref} changing from 12 to 15 V at $t_{\text{step}} = 10$ msec. The transfer function of the filter is given by

$$H(s) = K_C \frac{1 + s/\omega_z}{1 + s/\omega_p}, \quad (80)$$

where $K_C = 4.551 \times 10^3$, $\omega_z = 6.492 \times 10^3$ rad/s, and $\omega_p = 6.081 \times 10^5$ rad/s. For simulation of the circuit using the ELEX-RKF scheme, we rewrite $H(s)$ as

$$H(s) = K_C \left[(\omega_p/\omega_z) + \frac{K}{1 + s/\omega_p} \right], \quad (81)$$

where $K = (1 - \omega_p/\omega_z)$. The control block can now be implemented as shown in Fig. 20.

As in the previous example, at each stage of the RKF method, we solve the electrical equations ($\mathbf{A} \mathbf{x} = \mathbf{b}$), followed by updating the control block variables, and then proceed to the next RKF stage. The control block variables are treated by first upgrading the two integrator outputs. For example, in RKF stage 2, we would have

$$x_4^{(2)} = x_{4,n} + h\beta_{2,1} x_{3,n}, \quad (82)$$

$$x_9^{(2)} = x_{9,n} + h\beta_{2,1} x_{8,n}, \quad (83)$$

and limit $x_9^{(2)}$ as $0 \leq x_9^{(2)} \leq 1$. Next, we update the $V_{\text{ref}}^{(2)}$ and $x_{\text{tri}}^{(2)}$ (sawtooth) source values at $(t_n + \alpha_2 h)$, and then compute the remaining control variables as,

$$x_1^{(2)} = V_{\text{ref}}^{(2)} - V_{fb}^{(2)}, \quad (84)$$

$$x_5^{(2)} = \omega_p x_4^{(2)}, \quad (85)$$

$$g^{(2)} = 1 \quad \text{if } x_9^{(2)} > x_{\text{tri}}, \\ g^{(2)} = 0 \quad \text{otherwise}, \quad (86)$$

$$x_2^{(2)} = K \omega_p x_1^{(2)}, \quad (87)$$

$$x_6^{(2)} = \frac{\omega_p}{\omega_z} x_1^{(2)} \quad (88)$$

$$x_3^{(2)} = x_2^{(2)} - x_5^{(2)}, \quad (89)$$

$$x_7^{(2)} = x_6^{(2)} + x_4^{(2)}, \quad (90)$$

$$x_8^{(2)} = K_C x_7^{(2)}. \quad (91)$$

Fig. 21 shows $V_{\text{ref}}(t)$ and $V_{fb}(t)$, and Fig. 22 shows the gate pulses produced by the controller when V_{ref} changes from 12 V to 15 V at $t = t_{\text{step}}$.

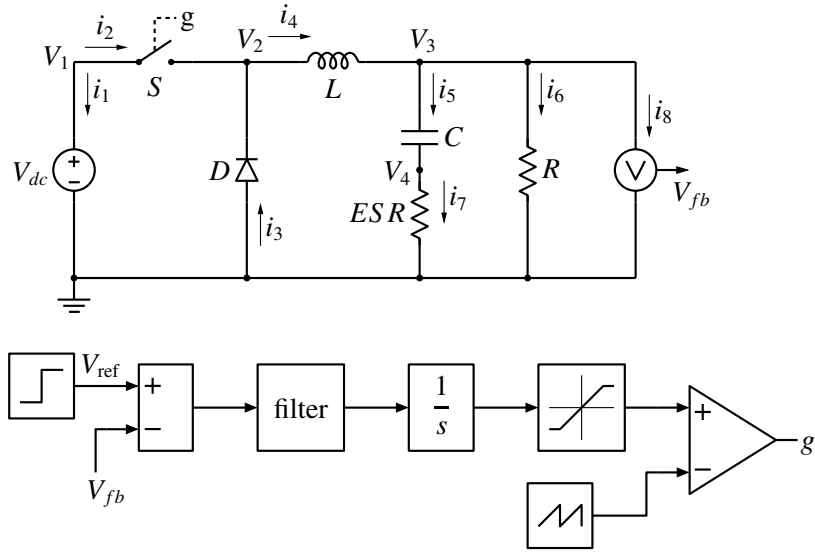


Figure 19: Buck converter circuit and control block. The circuit parameters are $V_{dc} = 25$ V, $C = 500 \mu\text{F}$, $L = 24 \mu\text{H}$, $R = 4 \Omega$, $ESR = 0.08 \Omega$. The sawtooth waveform has minimum and maximum values of 0 and 1, respectively, and frequency of 400 kHz.

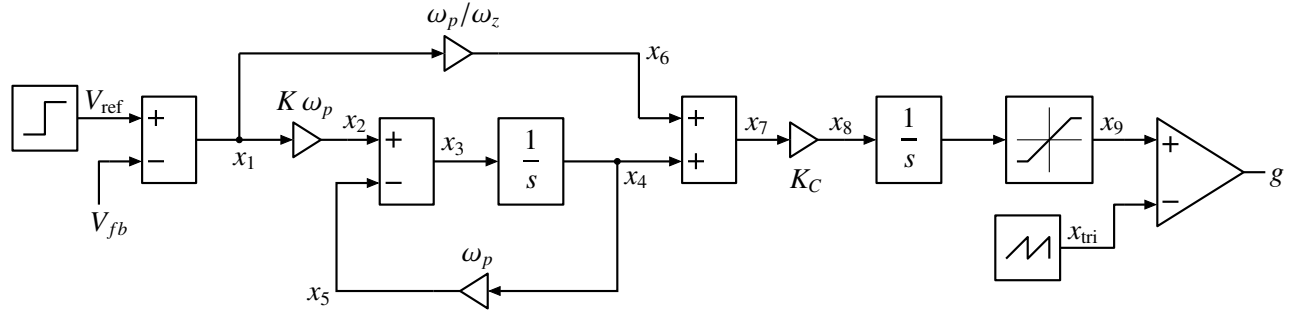


Figure 20: ELEX-RKF implementation of the control block of the voltage controlled buck converter of Fig. 19.

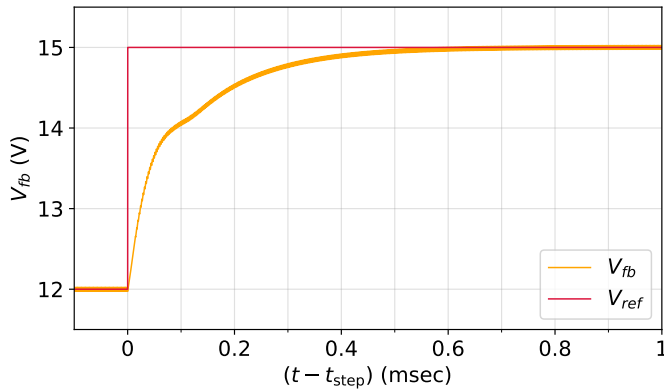


Figure 21: Plot of $V_{fb}(t)$ as obtained with the ELEX-RKF scheme for the voltage controlled buck converter of Fig. 19.

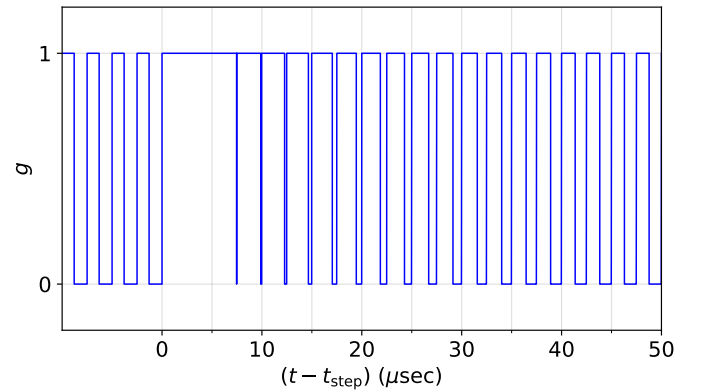


Figure 22: Plot of gate signal as obtained with the ELEX-RKF scheme for the voltage controlled buck converter of Fig. 19.

6 Conclusions and future work

In summary, we have presented a methodology called ELEX-RKF for using explicit methods – in particular

the RKF method – for simulation of power electronic circuits, considering the switches to be ideal. The reasons for higher simulation speed of the ELEX-RKF scheme as compared to implicit schemes are explained. Several challenges which are encountered in implementing the ELEX-RKF scheme are pointed out. With the help of suitable examples, these issues are illustrated, and techniques are described for resolving the same. Simulation results obtained using the ELEX-RKF scheme are presented for a few representative power electronic circuits.

The following future work is planned.

1. The ELEX-RKF scheme will be implemented in the open-source simulation package GSEIM [12], [13]. At the time of writing, GSEIM allows only implicit methods for electrical circuits, together with MNA for circuit equation formulation. Incorporation of the ELEX-RKF option will make GSEIM more versatile, and particularly useful for circuits which take a substantial amount of time with implicit methods.
2. PLECS [7] uses the Dormand-Prince (DP) 4-5 pair for solving the ODEs. Implementation of the DP method is conceptually very similar to the RKF method. It is envisaged that GSEIM will allow both ELEX-RKF and ELEX-DP options to the user.
3. In this work, we have not compared simulation times of the ELEX-RKF scheme with implicit methods. In future, we plan to use GSEIM to make such a comparison for typical power electronic circuits, thus enabling the user to make an informed choice about the solution method.

References

- [1] P. Nenzi, “NGSPICE circuit simulator release 26, 2014.”
- [2] PSIM. [Online]. Available: <https://powersimtech.com/products/psim/capabilities-applications/>
- [3] PSCAD. [Online]. Available: <https://www.pscad.com/>
- [4] M.B. Patil, V. Ramanarayanan, V.T. Ranganathan, *Simulation of power electronic circuits*. New Delhi: Narosa, 2009.
- [5] R.L. Burden and J.D. Faires, *Numerical Analysis*. Singapore: Thomson, 2001.
- [6] Dormand-Prince method. [Online]. Available: https://en.wikipedia.org/wiki/Dormand%E2%80%9993Prince_method
- [7] PLECS 4.6. [Online]. Available: <https://www.plexim.com/products/plecs>
- [8] W.J. McCalla, *Fundamentals of Computer-Aided Circuit Simulation*. Boston: Kluwer Academic Publishers, 1987.
- [9] M.B. Patil. SEQUEL Users’ Manual: Part-1. [Online]. Available: <http://www.ee.iitb.ac.in/~sequel>
- [10] GSEIM users manual. [Online]. Available: <https://gseim.github.io/build/html/index.html>
- [11] M. B. Patil, R. D. Korgaonkar, and K. Appaiah, “GSEIM: a general-purpose simulator with explicit and implicit methods,” *Sādhanā*, vol. 46, no. 4, pp. 1–13, 2021.
- [12] M.B. Patil, V.V.S. Pavan Kumar Hari, Ruchita D. Korgaonkar, and Kumar Appaiah, “An open-source simulation package for power electronics education,” available at <https://arxiv.org/abs/2204.12924>.
- [13] GSEIM. [Online]. Available: <https://github.com/gseim/gseim>